

# CO<sub>2</sub> laser induced long period gratings in optical microfibers

Haifeng Xuan<sup>1</sup>, Wei Jin<sup>1\*</sup>, Min Zhang<sup>2</sup>

<sup>1</sup>Department of Electrical Engineering, The Hong Kong Polytechnic University, Hong Kong

<sup>2</sup>Department of Electronic Engineering, Tsinghua University, Beijing, China

\*ewjin@polyu.edu.hk

**Abstract:** Long period gratings (LPGs) are fabricated by use of focused high frequency CO<sub>2</sub> laser pulses to periodically modify the transverse dimension of silica microfibers. A 20-period LPG with a 27dB attenuation dip is realized in a microfiber with a diameter of ~6.3μm. The resonant wavelength has a negative temperature coefficient and a high sensitivity to external refractive index. The microfiber LPGs may be useful in micron scale in-fiber devices and sensors.

©2009 Optical Society of America

**OCIS codes:** (060.2310) Fiber optics; (060.2370) Fiber optic sensors; (060.2280) Fiber design and fabrication; (230.3990) Micro-optical devices; (050.2770) Gratings

---

## References and links

1. A. M. Vengsarkar, J. R. Pedrazzani, J. B. Judkins, P. J. Lemaire, N. S. Bergano, and C. R. Davidson, "Long-period fiber-grating-based gain equalizers," *Opt. Lett.* **21**(5), 336–338 (1996).
2. V. Bhatia, and A. M. Vengsarkar, "Optical fiber long-period grating sensors," *Opt. Lett.* **21**(9), 692–694 (1996).
3. Y.-P. Wang, L. Xiao, D. N. Wang, and W. Jin, "Highly sensitive long-period fiber-grating strain sensor with low temperature sensitivity," *Opt. Lett.* **31**(23), 3414–3416 (2006).
4. P. Steinvurzel, E. D. Moore, E. C. Mägi, B. T. Kuhlmeier, and B. J. Eggleton, "Long period grating resonances in photonic bandgap fiber," *Opt. Express* **14**(7), 3007–3014 (2006).
5. Y. Wang, W. Jin, J. Ju, H. Xuan, H. L. Ho, L. Xiao, and D. Wang, "Long period gratings in air-core photonic bandgap fibers," *Opt. Express* **16**(4), 2784–2790 (2008).
6. I. K. Hwang, S. H. Yun, and B. Y. Kim, "Long-period fiber gratings based on periodic microbends," *Opt. Lett.* **24**(18), 1263–1265 (1999).
7. C. Y. Lin, G. W. Chern, and L. A. Wang, "Periodical corrugated structure for forming sampled fiber Bragg grating and long-period fiber grating with tunable coupling strength," *J. Lightwave Technol.* **19**(8), 1212–1220 (2001).
8. Y. Kondo, K. Nouchi, T. Mitsuyu, M. Watanabe, P. G. Kazansky, and K. Hirao, "Fabrication of long-period fiber gratings by focused irradiation of infrared femtosecond laser pulses," *Opt. Lett.* **24**(10), 646–648 (1999).
9. M. Sumetsky, "Basic elements for microfiber photonics: Micro/nanofibers and microfiber coil resonators," *J. Lightwave Technol.* **26**(1), 21–27 (2008).
10. L. M. Tong, R. R. Gattass, J. B. Ashcom, S. L. He, J. Y. Lou, M. Y. Shen, I. Maxwell, and E. Mazur, "Subwavelength-diameter silica wires for low-loss optical wave guiding," *Nature* **426**(6968), 816–819 (2003).
11. L. M. Tong, J. Y. Lou, R. R. Gattass, S. L. He, X. W. Chen, L. Liu, and E. Mazur, "Assembly of silica nanowires on silica aerogels for microphotonic devices," *Nano Lett.* **5**(2), 259–262 (2005).
12. G. Brambilla, V. Finazzi, and D. J. Richardson, "Ultra-low-loss optical fiber nanotapers," *Opt. Express* **12**(10), 2258–2263 (2004).
13. L. M. Tong, J. Y. Lou, and E. Mazur, "Single-mode guiding properties of subwavelength-diameter silica and silicon wire waveguides," *Opt. Express* **12**(6), 1025–1035 (2004).
14. J. Villatoro, and D. Monzón-Hernández, "Fast detection of hydrogen with nano fiber tapers coated with ultra thin palladium layers," *Opt. Express* **13**(13), 5087–5092 (2005).
15. J. C. Knight, G. Cheung, F. Jacques, and T. A. Birks, "Phase-matched excitation of whispering-gallery-mode resonances by a fiber taper," *Opt. Lett.* **22**(15), 1129–1131 (1997).
16. K. J. Vahala, "Optical microcavities," *Nature* **424**(6950), 839–846 (2003).
17. G. Kakarantzas, T. E. Dimmick, T. A. Birks, R. Le Roux, and P. S. J. Russell, "Miniature all-fiber devices based on CO(2) laser microstructuring of tapered fibers," *Opt. Lett.* **26**(15), 1137–1139 (2001).
18. W. Ding, S. R. Andrews, and S. A. Maier, "Modal coupling in surface-corrugated long-period-grating fiber tapers," *Opt. Lett.* **33**(7), 717–719 (2008).
19. J. D. Love, W. M. Henry, W. J. Stewart, R. J. Black, S. Lacroix, and F. Gonthier, "Tapered single-mode fibres and devices. I. Adiabaticity criteria," *IEE Proc. J.* **138**, 343–354 (1991).
20. H. F. Xuan, W. Jin, J. Ju, Y. P. Wang, M. Zhang, Y. B. Liao, and M. H. Chen, "Hollow-core photonic bandgap fiber polarizer," *Opt. Lett.* **33**(8), 845–847 (2008).

21. D. Östling, and H. E. Engan, "Narrow-band acousto-optic tunable filtering in a two-mode fiber," *Opt. Lett.* **20**(11), 1247–1249 (1995).
22. C. Y. H. Tsao, D. N. Payne, and W. A. Gambling, "Modal characteristics of three-layered optical fiber waveguides: a modified approach," *J. Opt. Soc. Am. A* **6**(4), 555–563 (1989).
23. Y.-J. Rao, Y.-P. Wang, Z.-L. Ran, and T. Zhu, "Novel Fiber-Optic Sensors Based on Long-Period Fiber Gratings Written by High-Frequency CO<sub>2</sub> Laser Pulses," *J. Lightwave Technol.* **21**(5), 1320–1327 (2003).
24. J. S. Petrovic, H. Dobb, V. K. Mezentsev, K. Kalli, D. J. Webb, and I. Bennion, "Sensitivity of LPGs in PCFs fabricated by an electric arc to temperature, strain, and external refractive index," *J. Lightwave Technol.* **25**(5), 1306–1312 (2007).
25. Z. B. Tian, S. S. H. Yam, and H. P. Loock, "Refractive index sensor based on an abrupt taper Michelson interferometer in a single-mode fiber," *Opt. Lett.* **33**(10), 1105–1107 (2008).
26. Z. B. Tian, S. S. H. Yam, J. Barnes, W. Bock, P. Greig, J. M. Fraser, H. P. Loock, and R. D. Oleschuk, "Refractive index sensing with Mach-Zehnder interferometer based on concatenating two single-mode fiber tapers," *IEEE Photon. Technol. Lett.* **20**(8), 626–628 (2008).
27. I. Del Villar, I. R. Matias, and F. J. Arregui, "Enhancement of sensitivity in long-period fiber gratings with deposition of low-refractive-index materials," *Opt. Lett.* **30**(18), 2363–2365 (2005).
28. V. P. Minkovich, J. Villatoro, D. Monzón-Hernández, S. Calixto, A. B. Sotsky, and L. I. Sotskaya, "Holey fiber tapers with resonance transmission for high-resolution refractive index sensing," *Opt. Express* **13**(19), 7609–7614 (2005).

---

## 1. Introduction

The development of long period gratings (LPGs) has made a significant impact in optical fiber communication [1] and sensors [2]. LPGs have been fabricated in conventional single mode fibers (SMFs) [2], index-guiding photonic crystal fibers (PCFs) [3], solid-core photonic bandgap fibers (PBFs) [4], and hollow-core PBFs [5]. These fibers have diameters of around 100 $\mu\text{m}$  and the techniques used for LPG fabrication in such fibers include UV laser exposure [2], Electric arc [6], chemical etching [7], and irradiation by femtosecond laser pulses [8] and CO<sub>2</sub> lasers [3,5].

Recently, micro/nanofiber photonic devices have attracted significant attention. It has been suggested that micro/nanofibers could function as the basic element in micro/nano photonics, which focus on micro photonic circuits that are composed of micro/nanofibers [9–11]. The optical micro/nanofibers can be taper-drawn from standard optical fibers and have potential of being used as low-loss micro/nano scale optical waveguides [10,12]. The micro/nanofibers have high fractional evanescent fields in air [13], allowing strong evanescent wave coupling between micro/nanofibers and their environment, and hence the straightforward applications are evanescent wave sensors [14] and waveguide couplers [15,16]. However, most of micro/nanofiber devices reported so far are assembled through waveguide coupling (e.g., coiling a micro/nanofiber, or placing two micro/nanofibers in close contact), which intensively made use of the high fraction of the external evanescent field of the micro/nanofibers.

There have been reports on fabricating LPGs in tapered SMFs with diameters of  $\sim 15\mu\text{m}$  by using a CO<sub>2</sub> laser irradiation method [17] and a lithography method [18]; however, the diameter of the tapered fibers are significantly larger than the optical wavelength and the fiber may not be considered as a microfiber.

In this paper, we report the fabrication of microfiber LPGs by using a low cost pulsed CO<sub>2</sub> laser system. The microfibers have diameter down to  $\sim 6\mu\text{m}$  and are taper-drawn from a conventional SMF. The LPGs are fabricated by periodically tapering the microfiber longitudinally by use of the focused CO<sub>2</sub>-laser pulses. We show that a 20-period LPG with a 27dB attenuation dip can be realized in such a microfiber. The microfiber LPG is found to have a negative temperature coefficient and a very high sensitivity to external refractive index. The paper is organized as follows: the fabrication of microfiber LPGs is outlined in Section 2, the modal property of and mode-coupling induced by LPG in the microfiber are described in Section 3, and the responses of the LPG to surrounding temperature and external refractive index are presented in Section 4.

## 2. Fabrication of LPG

The microfibers used in our experiments are drawn by tapering SMFs with a commercial coupler fabrication station. A commercial SMF-28 fiber (outer diameter  $D \sim 125 \mu\text{m}$ , core diameter  $d \sim 8.2 \mu\text{m}$ ,  $\Delta n \sim 0.36\%$ ) is used and pulled to the scale of a few microns. The SMF-28 fiber is heated and softened by a hydrogen flame, whose dimension along the fiber is  $\sim 8 \text{mm}$ . The flame torch is scanned along the fiber, while the two translation stages holding the fiber are symmetrically moved apart. With proper fabrication parameters, microfibers with diameter from hundreds of nanometers to a few micrometers and effective waist lengths of longer than  $\sim 30 \text{mm}$  can be fabricated. Since a microfiber (the waist of taper) is adiabatically taper-pulled from a SMF, it is automatically connected to its SMF pigtails. This guarantees that the fundamental  $\text{HE}_{11}$  mode of the microfiber is excited with approaching 100% efficiency while other modes of the microfiber are largely not excited [19].

Figure 1 shows the experimental setup for fabricating LPG in microfibers. The two SMF pigtails of the microfiber are respectively connected to a Light-Emitting Diode (LED) and an optical spectrum analyzer (OSA). The  $\text{CO}_2$  laser is adjusted to have the following parameters: pulses width  $2.0 \mu\text{s}$ , repetition rate  $10 \text{kHz}$ , and average power  $\sim 0.02 \text{W}$ . This power level is significantly smaller than the one used for LPG fabrication in normal-size optical fibers [5,20]. The  $\text{CO}_2$  beam is focused to a spot with  $\sim 30 \mu\text{m}$  in diameter and has a  $\sim 50 \mu\text{m}$  depth of focus, and the size of focal spot is considerably larger than the diameter of the microfiber. The focused beam can be scanned, via a computer controlled two-dimensional optical scanner, transversely and longitudinally as instructed by a preprogrammed routing. During the fabrication, the laser beam is firstly scanned transversely across the microfiber and then moved longitudinally by a step of grating pitch (e.g.  $\Lambda \sim 100 \mu\text{m}$ ) to have a second scan. This procedure is repeated for  $N$  times in order to fabricate a LPG with  $N-1$  periods. The process of making  $N$  successive transverse scans is called one scanning cycle. By controlling the number of scanning cycles, the depth of the attenuation dip in the transmission may be controlled.

During scanning, the high-frequency  $\text{CO}_2$  laser pulses hit repeatedly on the microfiber and induce a local high temperature to soften the silica of the fiber. By applying a small weight as shown in Fig. 1, a small constant longitudinal tensile strain is induced and the soften region, i.e., the  $\text{CO}_2$  laser hit region, of the microfiber will be drawn slightly, which creates a micro-taper. Figure 2(a) shows the microscope image of periodical micro-tapers created on a microfiber with a diameter of  $6.3 \mu\text{m}$  after 15 scanning cycles. Figures 2(b) and 2(c) are respectively the microscope and SEM images of a micro-tapered region. The diameter of micro-taper waist shown in the Figs. 2(b) and 2(c) is  $\sim 65$  percent of microfiber, while the length of micro-taper is  $\sim 35 \mu\text{m}$ .

Figure 3 shows the measured transmitted spectrum of a LPG made in a microfiber with diameter of  $\sim 6.3 \mu\text{m}$ . The grating has a pitch of  $\sim 100 \mu\text{m}$  and 20 periods. The insertion loss of LPG is less than  $\sim 0.8 \text{dB}$  and could be further reduced by optimizing the fabrication parameters. As shown in the inset of Fig. 3, the 3dB-bandwidth of attenuation dip is  $\sim 2 \text{nm}$ , much narrower than that of the LPGs in conventional SMFs [1], index-guiding PCFs [3], and hollow core PBFs [5]. The narrower bandwidth may be explained as follows: the 3dB-bandwidth of a LPG may be expressed as [21]

$$\Delta\lambda_{3dB} \propto \frac{\Lambda^2(\lambda_0)}{L} \left| \frac{d\Lambda}{d\lambda} \right|^{-1} \quad (1)$$

where  $L$  is the length and  $\Lambda$  is the pitch of the LPG at the phase matching wavelength  $\lambda_0$ . As will be seen from the discussion in section 3, the grating pitch  $\Lambda(\lambda_0)$  is smaller while  $d\Lambda/d\lambda$  is bigger for microfibers than for conventional SMFs, the 3dB bandwidth is then expected to be smaller.

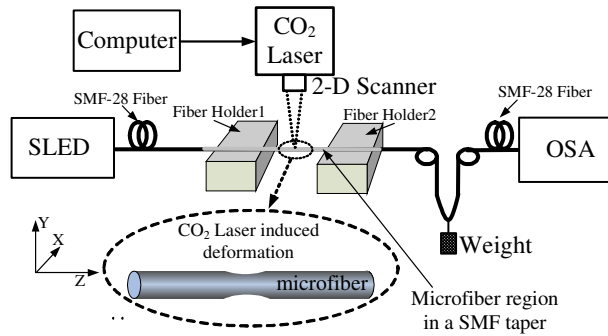


Fig. 1. Schematic of the CO<sub>2</sub> laser system for fabricating LPGs in microfibers.

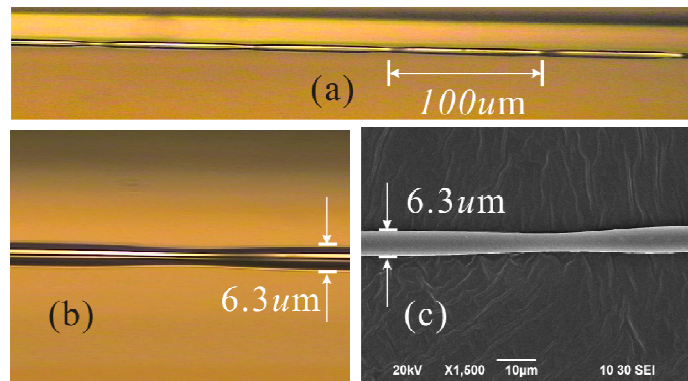


Fig. 2. A LPG fabricated in a microfiber. (a) Microscope image showing the periodic microtapers along the fiber. (b) Microscope and (c) SEM images showing the details of two microtapers made on a 6.3µm diameter microfiber.

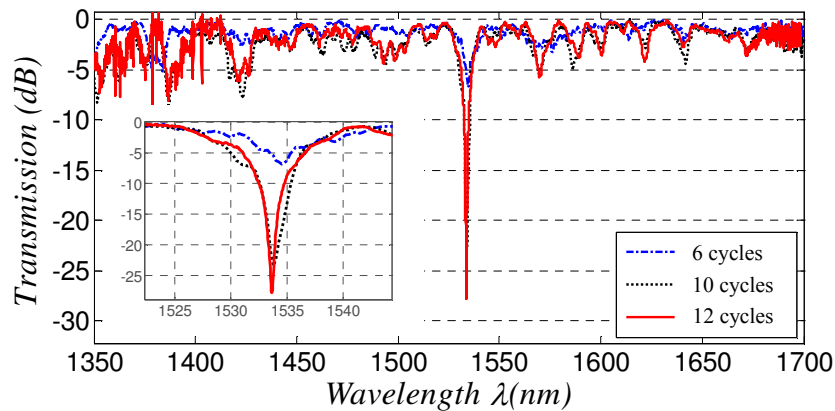


Fig. 3. Evolution of the transmitted spectrum of a LPG in a microfiber with increasing number of scanning cycles (6th, 10th, and 12th). The LPG is written in a ~6.3µm diameter microfiber and has 20 periods and a grating pitch of 100µm.

### 3. Mode property and mode-couplings by LPG

The mode property of a microfiber can be studied readily by solving the Maxwell equations for a uniform, cylindrically symmetric multilayer dielectric waveguide. Either a two-layer (i.e., a circular silica rod with an infinite air clad) or a three-layer (a Ge-doped central region, a

silica ring region and an infinite air clad) step-index model [22] may be used. For the microfibers interested in this paper, the Ge-doped region has a diameter of  $\sim 0.4\mu\text{m}$  or less and a refractive index  $\sim 0.36\%$  higher than that of fused silica. The results from the two- and three-layers models are very close. In the following, the two-layer model is adopted to investigate the modal characteristics of the microfibers. Figure 4(a) shows the effective index  $n_{\text{eff}}$  of the first six modes in air clad silica microfibers as function of normalized fiber diameter  $D/\lambda$ . As shown in Fig. 4(a), for  $D/\lambda > 0.73$ , the microfiber is a multi-mode waveguide. Around  $D/\lambda \sim 4$ , which is the diameter of the microfibers used for fabricating the LPG shown in the Figs. 2 and 3, the microfiber can support dozens of modes. Hence, by introducing a LPG satisfying the phase matching condition given in Eq. (2), resonant mode coupling devices may be implemented.

$$\Lambda = \lambda / (n_{\text{eff},0} - n_{\text{eff},v}) \quad (2)$$

where  $\lambda$  is the resonant wavelength,  $\Lambda$  is the grating pitch, and  $n_{\text{eff},0}$  and  $n_{\text{eff},v}$  are respectively the effective refractive indices of the fundamental and the  $v$ -order mode. Figure 4(b) shows the calculated grating pitches as functions of wavelength for mode coupling between  $\text{HE}_{11}$  and higher-order modes including the  $\text{LP}_{11}$  group (i.e.,  $\text{TE}_{01}$ ,  $\text{HE}_{21}$ , and  $\text{TM}_{01}$ ),  $\text{LP}_{21}$  group (i.e.,  $\text{HE}_{31}$ , and  $\text{EH}_{11}$ ) and  $\text{LP}_{02}$  ( $\text{HE}_{12}$ ) for a  $6.3\mu\text{m}$  diameter microfiber. For a grating pitch of  $\sim 100\mu\text{m}$ , Fig. 4(b) predicts that resonant mode coupling from  $\text{LP}_{01}$  ( $\text{HE}_{11}$ ) to the  $\text{LP}_{11}$  group would occur around optical wavelength  $1.5\mu\text{m}$ , and this prediction is experimentally confirmed by the results shown in Fig. 3.

As can be seen from Fig. 4(a), the refractive index difference between fundamental and higher-order modes in a microfiber is much larger than that in conventional SMFs. For example, the index differences between fundamental  $\text{HE}_{11}$  and the higher order modes are about  $\sim 0.016$  for  $\text{LP}_{11}$  group ( $\text{TE}_{01}$ ,  $\text{HE}_{21}$ , and  $\text{TM}_{01}$ ),  $\sim 0.038$  for  $\text{LP}_{21}$  group ( $\text{HE}_{31}$ , and  $\text{EH}_{11}$ ) and  $0.046$  for  $\text{LP}_{02}$  ( $\text{HE}_{12}$ ) in a microfiber with a diameter of  $D \sim 4\lambda$ ; while the difference between the  $\text{HE}_{11}$  and a cladding mode in a conventional SMF is  $\sim 0.003$ . According to Eq. (2), this large index difference will require a much smaller grating pitch to achieve phase matching. Figure 5 show the phase matching ( $\Lambda-\lambda$ ) curves of microfibers with different diameters. The phase matching conditions between the fundamental and the  $\text{HE}_{21}$  modes are shown in Fig. 5(a), while Fig. 5(b) shows the phase matching conditions between the fundamental and the  $\text{HE}_{12}$  modes.

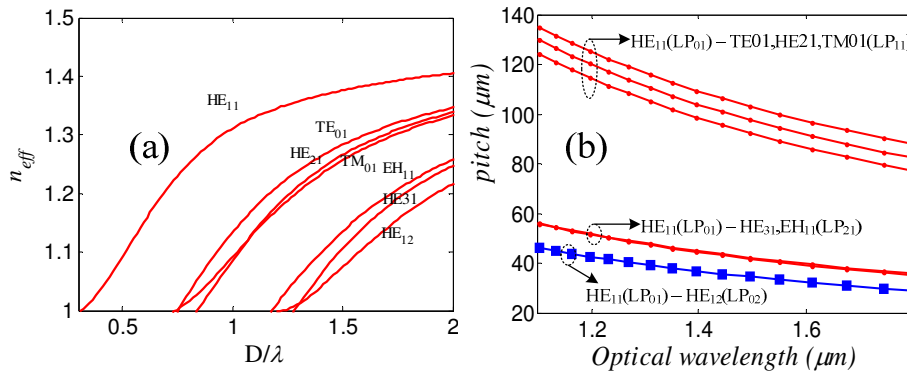


Fig. 4. Wave guiding properties of air clad silica optical microfibers. (a) Effective refractive index  $n_{\text{eff}}$  of guided modes as functions of the normalized fiber diameter  $D/\lambda$ ; (b) Grating pitches as function of wavelength for modes coupling between  $\text{HE}_{11}(\text{LP}_{01})$  and higher-order modes. This fiber diameter is assumed to be  $6.3\mu\text{m}$ .

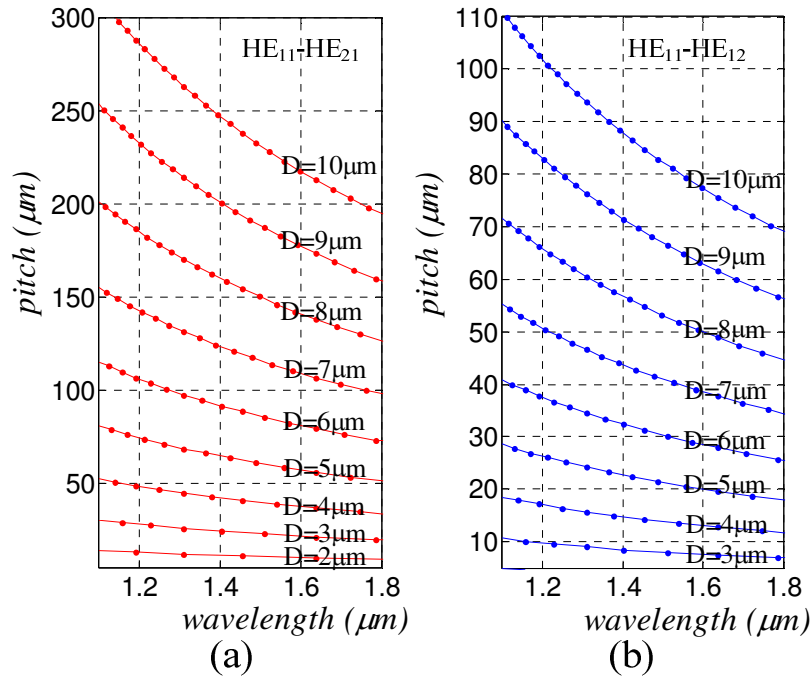


Fig. 5. Phase matching curves for microfibers with different diameter  $D$ . (a) Coupling between  $HE_{11}$  and  $HE_{21}$ ; (b) Coupling between  $HE_{11}$  and  $HE_{12}$ .

#### 4. Response of microfiber LPG to temperature and refractive index

The responses of microfiber LPGs to temperature and external refractive index are experimentally studied and the results are shown in Figs. 6 and 7, respectively. For temperature response, the transmission spectrum is monitored when temperature surrounding the microfiber LPG is varied from 25 to 100°C by use of a digitally controlled oven. The resonance dip around 1530nm blue-shifts with increasing temperature (Fig. 6(a)) and the relationship between the dip wavelength and temperature is shown in Fig. 6(b), corresponding to a temperature coefficient of  $\sim -130\text{pm}/^\circ\text{C}$ . The magnitude of this temperature coefficient is similar to or slightly bigger than that of the LPGs in standard SMF-28 fiber [2,23], and  $\sim 30$  times larger than that of the LPGs in the index guiding PCFs [3] or air-core PBFs [5]. It's noticed that resonant wavelength has a negative temperature coefficient, which is opposite to LPGs in conventional SMFs.

To understand negative temperature coefficient, we consider the generic expression of temperature response of a LPG [24]:

$$\frac{d\lambda}{dT} = \gamma \left( \frac{d\Lambda}{dT} \Delta n_{eff} + \frac{d\Delta n_{eff}}{dn} \frac{dn}{dT} \Lambda \right) \quad (3)$$

in which  $n$  and  $\Delta n_{eff} = n_{eff,0} - n_{eff,v}$  are respectively refractive index of waveguide and refractive index difference between coupled modes.  $\gamma$  describes the waveguide dispersion and defined by  $\gamma = (1/\Delta n_{eff})(d\lambda/d\Lambda)$ . The terms  $d\Lambda/dT$  and  $dn/dT$  are respectively the thermal expansion and thermo-optic coefficients of the silica material, and they are all positive. For a microfiber, as the fundamental mode has a larger percentage of power in silica than the higher order mode,  $d\Delta n_{eff}/dn$  should also be positive. The crucial factor that

determines the sign of the temperature response is then  $\gamma = (1/\Delta n_{eff})(d\lambda/d\Lambda)$ . As can be seen from Fig. 5,  $d\lambda/d\Lambda$  is negative. This results in a negative  $\gamma$  and hence a negative temperature coefficient.

We also observed changes in the depth and width of the resonant peak during experiments (see Fig. 6(a)). We are not sure about the causes behind this but it could be due to bend induced chirping effect. We actually observed movement of the microfiber during experiment. Further investigation on this aspect is needed.

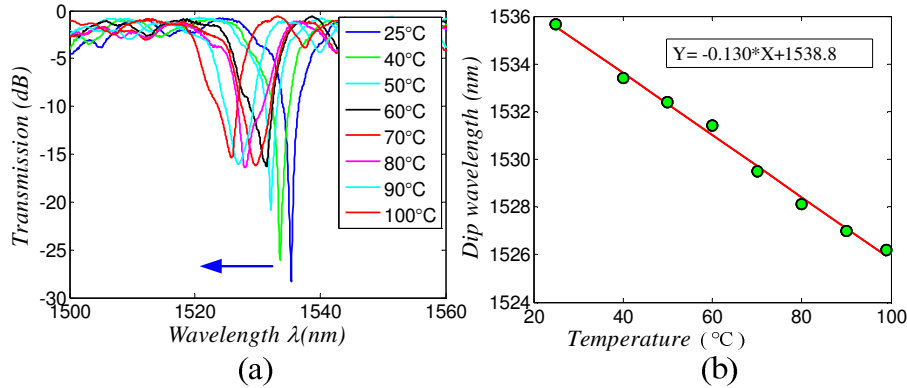


Fig. 6. (a) Shift of LPG resonance dip around 1536nm with temperature; (b) Linear fit showing the relationship between the resonant wavelength and temperature. The LPG used is the one shown in Figs. 2 and 3.

The response of the microfiber LPG to external refractive index is measured by immersing the microfiber section (the center part of the SMF28 tapered region) containing the LPG into calibrated Gargille refractive index oils and monitoring the shifts of resonance dips by using an OSA. It's noted that an air clad microfiber LPG with nice resonant dips in a particular wavelength range does not always show resonance dips in the same wavelength range when it is immersed into refractive index oil. This is because that the mode and dispersion characteristics of a liquid clad microfiber are different from that of air clad microfiber and, in fact, a liquid clad microfiber should guide a fewer modes than an air clad microfiber. However, by careful selecting the microfiber and LPG parameters and inducing strong waveguide modulation as shown in Fig. 2, it is possible to produce a higher order gratings with resonant dips located within our wavelength of interest.

Figure 7 shows the response of a LPG to external refractive index. The LPG has 20 periods LPG and a grating pitch of 120 $\mu$ m and is written in a microfiber with a diameter of  $\sim$ 7.4 $\mu$ m. The transmitted spectrums of the microfiber LPG before and after it is immersed into a refractive index oil ( $n = 1.32$  at 25 degree Celsius) are shown in Fig. 7(a). The resonant dips in the transmission spectrum for the liquid clad fiber are believed to be due to coupling to different cladding modes ( $HE_{31}$ ,  $EH_{11}$  or  $HE_{12}$ ) by a second order grating. Figure 7(b) shows the shift of the resonant dip around 1355nm with external refractive index variation. The refractive index variation was achieved by heating a refractive index oil with a calibrated index of  $n_D = 1.320$  at 25 degree Celsius. The measured dip wavelengths as function of external refractive index variation (achieved by heating) and the corresponding linear fit are illustrated in Fig. 7(c) and marked as solid circle and solid lines, respectively. For comparison, the measured dip wavelength of the microfiber LPG when it is immersed into different oil with refractive index 1.315 is also shown in Fig. 7(c) and marked as a solid square. The results obtained by heating and by oil replacement differ only slightly with each other, indicating that the error due to thermal effect of the fiber material is very small. The refractive index coefficient is estimated to be  $\sim$ 1900nm/RI. This value is  $\sim$ 60 times bigger than an in-fiber Michelson interferometer made from abrupt taper of SMF [25] or a in-fiber Mach-

Zehnder interferometer based on concatenating two SMF tapers [26], 5 times bigger than a LPG specially designed for sensitivity enhancement [27], and comparable to and slightly smaller than a multi-mode interferometer abrupt microstructure fiber taper [28]. Assuming a 10pm resolution in wavelength measurement, a refractive index resolution of  $5.3 \times 10^{-6}$  would be achievable with the microfiber LPG.

To quantitatively determine the effect of temperature on the refractive index measurement, we numerically simulated the temperature induced shift of the resonance wavelength for a liquid clad microfiber with a diameter of  $7.4 \mu\text{m}$ . The microfiber contains a Ge-doped core of diameter  $0.49 \times 10^{-6} \mu\text{m}$  and is surrounded by an index oil with refractive index  $n_D = 1.32$  at  $25^\circ\text{C}$ . The temperature coefficient of refractive index oil is taken from the specification of the oil used in our experiment and equals to  $-0.000336/^\circ\text{C}$ . The thermo-optic coefficient of silica is taken as  $7.8 \times 10^{-6}/^\circ\text{C}$  and the thermo-optic coefficient of Ge-doped region is  $7.97 \times 10^{-6}/^\circ\text{C}$ . Three different cases are studied: (1) the indexes of microfiber are constant while the index of the surrounding oil varies with temperature; (2) the indexes of microfiber vary with temperature while the index of the surrounding oil is equal to  $n_D = 1.32$ ; (3) the indexes of both microfiber and surrounding oil vary with temperature. The temperature coefficients are respectively  $\sim 0.55 \text{ nm}/^\circ\text{C}$  for case (1),  $\sim 0.04 \text{ nm}/^\circ\text{C}$  for case (2), and  $\sim 0.58 \text{ nm}/^\circ\text{C}$  for case (3). Simulation results show that the error due to thermal effects of the fiber materials is  $\sim 7\%$ .

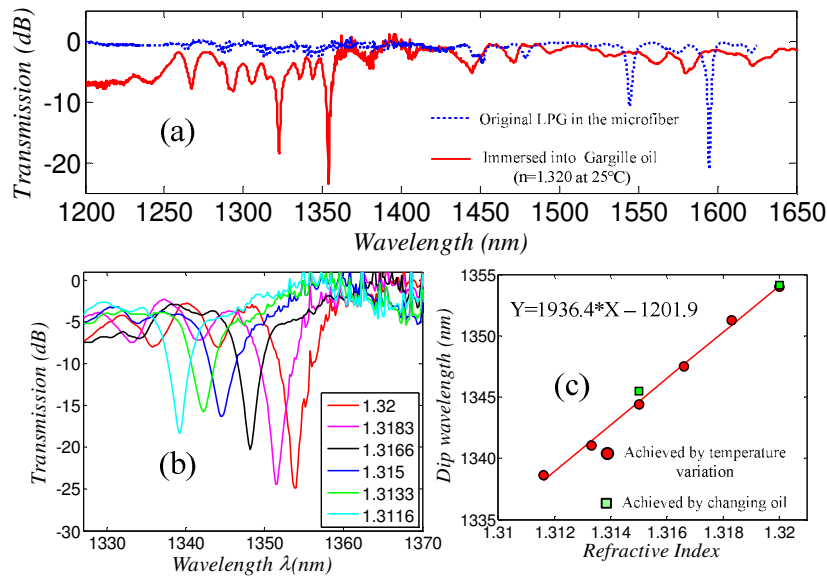


Fig. 7. The response of an LPG in a microfiber with a diameter of  $7.4 \mu\text{m}$  to external refractive index. (a) The transmitted spectrum of the LPG before and after it is immersed into a refractive index oil; (b) Dip wavelength as a function of refractive index (c) Linear fit showing the relationship between the dip wavelength and external refractive index. The LPG is written near the center of waist of the fiber taper. The diameter of the waist is  $\sim 7.4 \mu\text{m}$  and the length of the taper is  $\sim 20 \text{ mm}$ .

It should be mentioned that, before inscription of LPG, the transmission spectrum of a microfiber with SMF pigtailed at both ends is found almost not changing with variation of environment. However, we observed considerable change in the transmission spectrum in the microfiber sample with a LPG in it. This could be due to bending effect induced during the experimental process. We did observe movement of the microfibers with variation of environment (e.g., air current, acoustic vibration, etc.), but were not able to quantify it because of the difficulty in introducing bend with known curvature in such thin fibers. This would be a subject of future research.



## 5. Conclusion

Coupling between guided modes in microfibers are realized by fabricating LPGs along the microfibers. The microfibers are taper-drawn from conventional SMFs and the LPGs are fabricated by periodically inducing micro-tapers along the microfiber by use of focused pulsed CO<sub>2</sub>-laser in combination with small applied longitudinal tensile strain. We show that a 20-period LPG with 27dB resonant dip can be realized in a microfiber with the diameter of ~6.3μm. The response of such made microfiber LPGs to temperature was experimentally investigated. The resonance dip is found to shift toward short wavelength (blue shift) with increasing ambient temperature and has a sensitivity of ~-130pm/°C, while for most of LPGs in normal scale optical fiber, the resonant wavelength showed red-shift with temperature. The wavelength response of the microfiber LPG to external refractive index was also studied and found to be ~1900nm/RI, showing the microfiber FBG could be used as a very sensitive refractive index sensor.

## Acknowledgement

The research work was supported by the Research Grant Council of the Hong Kong SAR Government through a GRF grant PolyU5182/07E, and NSF of China though grant no: 60629401.